Effect of basic oxygen furnace slag type on carbon dioxide sequestration from landfill gas emissions

Krishna R. Reddy
Professor, University of Illinois at Chicago, Department of Civil & Materials Engineering, 842 West Taylor Street, Chicago, IL 60607, USA, e-mail: kreddy@uic.edu (Corresponding author)

Jyoti K. Chetri
Graduate Research Assistant, University of Illinois at Chicago, Department of Civil & Materials Engineering, 842 West Taylor Street, Chicago, IL 60607, USA, e-mail: jkc4@uic.edu

Girish Kumar
Graduate Research Assistant, University of Illinois at Chicago, Department of Civil & Materials Engineering, 842 West Taylor Street, Chicago, IL 60607, USA, e-mail: gkumar6@uic.edu

Dennis G. Grubb
President, Fugacity LLC, 126 Veronica Lane, Lansdale, PA 19446, USA;
e-mail: dggrubbphdpe@gmail.com

Manuscript Submitted to:
Waste Management

July 15, 2019

ABSTRACT

This study investigates the carbon dioxide (CO_2) sequestration potential of three different basic oxygen furnace (BOF) slags (IHE-3/15, IHE-9/17, and Riverdale) subjected to simulated landfill gas (LFG) conditions (50% CH_4 and 50% CO_2 v/v) in a series of batch and column experiments. Batch experiments were performed at different moisture contents (0%, 10%, 15% and 20% moisture by weight) and temperatures (7 ºC, 23 ºC and 54 ºC) to examine the effect of moisture and temperature on the CO_2 sequestration potential of the BOF slags. The column experiments were conducted under continuous humid gas flow conditions. The results from the batch experiments show that the CO_2 sequestration was significantly higher in a moist state (10%, 15%, 20% moisture (w/w)) versus the dry state (0% moisture). The optimum moisture content (w/w) for CO_2 sequestration was different for each BOF slag; IHE-3/15 (10%), IHE-9/17 (20%) and Riverdale (20%). The variation in ambient temperature did not show any significant effect on the CO_2 sequestration capacity of the BOF slags. The CO_2 sequestration capacity of IHE-3/15, IHE-9/17 and Riverdale BOF slags determined by long-term batch experiments were 105 mg/g, 80 mg/g and 67 mg/g, respectively. The IHE-3/15 slag demonstrated the highest carbonation potential and was attributed to its finer particle size and higher free lime, portlandite and larnite content. The IHE-9/17 and Riverdale slags showed significantly lower CO_2 sequestration capacity in comparison to the IHE-3/15 slag. The amount of free lime, portlandite and larnite, which are considered to be the most reactive minerals during carbonation, was nearly

1.3 times less than that of the IHE-3/15 slag in the IHE-9/17 and Riverdale slags. Also, the Riverdale slag showed relatively lower CO_2 sequestration in column experiment in comparison to the batch experiments, perhaps due to a high in-situ density which limited CO_2 diffusion and hence the CO_2 uptake. Overall, this study provides a means to analyze the suitability of the use of BOF slags in landfill covers for mitigating fugitive CO_2 emissions from landfills.

Keywords: Municipal solid waste; Landfill gas emissions; Landfill cover; Basic oxygen furnace slag; Carbon dioxide sequestration.

1. Introduction

Municipal solid waste (MSW) landfill gas emissions, especially methane (CH_4) and carbon dioxide (CO_2), constitute major contributors of anthropogenic greenhouse gas (GHG) emissions worldwide. Engineered MSW landfills are generally designed with active gas collection systems to capture the LFG emissions. Despite having the well-designed active gas collection systems, fugitive emissions persist. According to the United States Environmental Protection Agency (USEPA), there were approximately 2,000 active landfills in the U.S. in 2009 (USEPA, 2018). With a growing number and size of these landfills, the problem of fugitive LFG emissions is persistently exacerbating and transforming into an untenable challenge. In the recent years, many researchers have attempted to mitigate the landfill CH_4 emissions by proposing biocovers (Sadasivam and Reddy 2014). Biocovers are alternate cover systems containing organic matter to enhance microbial oxidation of CH_4, thus limiting the CH_4 emissions. Although a considerable amount of CH_4 emissions are mitigated, there are still large amounts of CO_2, resulting from CH_4 oxidation and MSW degradation, released into the atmosphere, leaving the problem of LFG emissions unresolved. Goldsmith Jr et al. (2012) have reported fugitive CH_4 emissions as a function of climate and cover type from their study in 20 landfills in the USA. For a final cover, highest CH_4 flux of 32 $g/m^2/d$ and an average CH_4 emission rates of 0.09 $g/m^2/d$ for a closed landfill with active gas collection system have been reported. Since LFG is composed of approximately 50% CH_4 and 50% CO_2 (USEPA, 2014), the corresponding CO_2 emission derived

78 from the CH_4 emissions data as mentioned earlier will be 88 $g/m^2/d$ and 0.25 $g/m^2/d$ for a landfill
79 with final cover without gas collection system and landfill with active gas collection,
80 respectively.

81 Several studies have been carried out and technologies have been developed to capture
82 CO_2 at industrial facilities that emit large amounts of CO_2 (e.g., power plants, manufacturing
83 plants). In this regard, mineral carbonation (MC) has proven to be a potential solution to CO_2
84 sequestration and safe means for the storage of CO_2 (Huijgen et al., 2005). Industrial alkaline
85 solid residues such as steel slag have shown a promising CO_2 sequestration potential (Huijgen et
86 al., 2005; Huijgen et al., 2006: Bonenfant et al., 2008; Lekakh et al., 2008; Chang et al, 2010;
87 Kunzler et al., 2011; van Zomeren et al., 2011; Pan et al., 2012). Steel slags are good source of
88 calcium rich alkali minerals and their low cost and high availability makes them appealing for
89 CO_2 sequestration applications. Among the different types of steel making slags (BF, BOF, EAF
90 and LF), BOF slags have highest carbonation potential due to high residual lime content (Chang
91 et al., 2010). BOF slag is formed during conversion of pig iron to steel. Superheated oxygen is
92 blown into the furnace containing molten iron, scrap metal, alloying agents and various fluxes
93 and approximately 20-25 wt% of Fe (0) is converted back to Fe(II, III), which accumulates in the
94 slag. This process is followed by air and/or water cooling of the molten BOF slag which
95 produces dense rock type material (National Slag Association, 2013) having a somewhat

vesicular morphology and array of crystallized and amorphous minerals, whose proportions are affected by rates of cooling.

The carbonation process in steel slag involves dissolution of CO_2 in water, leaching of Ca ions from the slag matrix, and precipitation of carbonates. Equations 1 to 4 show the basic reactions involved in carbonation of a BOF slag. Further detailed explanation on carbonation mechanism is given in Reddy et al. (2018a, b).

$$CaO + H_2O = Ca^{2+} + 2OH^- \quad (1)$$

$$Ca(OH)_2 = Ca^{2+} + 2OH^- \quad (2)$$

$$CO_2 + H_2O = CO_3^{2-} + 2H^+ \quad (3)$$

$$Ca^{2+} + CO_3^{2-} = CaCO_3 \quad (4)$$

The CO_2 sequestration potential of BOF slags depends upon various factors such as chemical composition, moisture content, temperature, particle size, and gas pressure (Huijgen et al., 2005; Baciocchi et al., 2009; van Zomeren et al., 2011). Although several studies have been carried out on BOF slags for use in CO_2 sequestration (Huijgen et al., 2005; van Zomeren et al., 2011; Su et al., 2016), none has focused on CO_2 sequestration under typical landfill conditions. **Table 1** summarizes some of the studies on BOF slag describing the research objectives and experimental conditions. For example, study by Huijgen et al. (2005) focuses on the mineral CO_2 sequestration of steel slag fines in a slurry condition (L/S ratio of 2 to 20 L/kg) at higher stirring rate (100- 2000 rpm), CO_2 pressure of 1-30 bar and temperature of 25-225 °C. The carbonation

115 conditions were optimized for maximum carbonation of the steel slag, and maximum
116 carbonation was obtained at 19 bar CO_2 pressure, 100 °C, slag particle size < 38 μm and in 30
117 minutes reaction time. Study by Sarperi et al. (2014), which is closest to our study, showed the
118 removal of CO_2 and H_2S simultaneously using BOF slag exposed to biogas generated from pilot
119 digester under atmospheric conditions. The key difference is that they used powder BOF slag
120 (particle size 0-1 mm) for column test in order to optimize CO_2 removal.

121 In general, none of the past studies have explored CO_2 sequestration potential of BOF
122 slag in landfill conditions. Furthermore, although, many studies have compared the carbonation
123 potential of different types of steel slag, our study is the first to analyze the heterogeneity of the
124 BOF slags based on their production batch, and its effect on their carbonation potential.

125 The objectives of the current study are 1) to analyze the variability that exists within the
126 BOF slag based on their production batch and plant; 2) to examine the effect of process variables
127 such as moisture and temperature on the carbonation potential of different BOF slags under
128 landfill conditions; 3) to investigate the governing mechanisms in carbonation of BOF slags in
129 landfill conditions. Batch and column experiments were conducted with three different BOF
130 slags to determine the carbonation potential of the slags under simulated landfill conditions. In
131 the landfill, it is difficult to optimize the carbonation conditions such as moisture content, gas
132 pressure, stirring rate etc. due to which it is of paramount importance to simulate the field
133 conditions as closely as possible.

2. Materials and methods

2.1. Materials

The BOF slags used in this study were obtained from the Indiana Harbor East (IHE) and Riverdale Steel Mills in Indiana and Illinois, respectively. The IHE BOF slags were sampled in March, 2015 and September, 2017 and the Riverdale BOF slag was sampled in September, 2017. The slag samples were received in a crushed granular form with top sieve size of 10 mm (3/8 inch). The BOF slags from IHE steel mill are denoted as *IHE-3/15* and *IHE-9/17* and the steel slag from Riverdale steel mill is denoted as *Riverdale*. A gas mixture of 50% CH_4 and 50% CO_2 by volume (Praxiar Distribution, Inc., Illinois) was used as simulated LFG for all the experiments performed in this study.

2.2. Characterization of slags

Particle size distribution was determined as per ASTM D422. The specific gravity, soil classification, and water holding capacity (WHC) were determined according to ASTM D584, D2487 and D2980, respectively. Loss on ignition (LOI) was determined per ASTM D2974.

153 Hydraulic conductivity was measured according to ASTM D2434 standard procedure using a
154 rigid wall permeameter. The pH and oxidation-reduction potential (ORP) were measured using
155 an ORION Model 720A pH meter at a liquid to solid ratio of 1:1. The pH meter was pre-
156 calibrated using standard buffer solutions of pH 4, 7 and 10 before use. Electrical conductivity
157 (EC) was measured using a Corning 311 Conductivity Meter pre-calibrated using standard
158 solution of 12.9 mS/cm before use. Acid neutralization capacity (ANC) and carbonate content
159 were determined according to ASTM STP-1123 (Isenburg and Moore, 1992) and ASTM D4373,
160 respectively.

161 The total elemental content analysis of IHE 3/15 and IHE 9/17 slags was conducted
162 through a combination of X-ray fluorescence (XRF) and solid phase acid digestion with
163 chemical analysis by inductively coupled plasma optical emission spectrometry (ICP-OES). The
164 total elemental content analysis of Riverdale slag sample was conducted using USEPA
165 SW3050B method with chemical analysis by inductively coupled plasma mass spectrometry
166 (ICP-MS). Leaching behavior of all three BOF slag samples were analyzed by performing
167 Toxicity Characteristic Leaching Procedure (TCLP) and Synthetic Precipitation Leaching
168 Procedure (SPLP) tests per EPA Method 1311 and1312 standard procedures.

169 Mineralogical composition of all three slag samples was determined by X-ray powder
170 diffraction (XRD) and Rietveld quantification analyses. For XRD, the sample was prepared by
171 grinding 3 g of sample using BICO Model VP-1989 mill with a 3.5 inch-ring and puck. XRD

data were collected by the Siemens D500 computer-automated diffractometer using Bragg-Brentano geometry. Quantitative analysis was performed using the whole pattern fitting function of Diffrac Plus Topas R, a proprietary Bruker AXS software (v. 2.0, 2000) which is based on Rietveld method (Rietveld 1969).

Morphological microstructure analyses were performed using scanning electron microscope (SEM). For SEM analysis, smaller grain mounds were prepared with slag samples before and after carbonation and sputter coated with 20 nm Pt/Pd using Cressington HR208 sputter coater to omit charging of particles during analysis. The SEM analyses were performed by JEOL JSM-6320F High Resolution Scanning Microscope operated at 2.5 kV.

2.3. Batch experiments

Batch experiments were performed on each as-received BOF slag under synthetic landfill gas conditions at different moisture contents and temperatures. Three different series of batch experiments were performed on each of the three BOF slags as follows:

- Series 1: These batch tests were performed to ass the effect of moisture content on CO_2 sequestration in 24 hours. For testing on each slag type, four 1 g oven dried slag samples were mixed with deionized water at specific moisture content (0%, 10%, 15% and 20%) in four 125 mL glass vials under normal atmospheric condition and purged with synthetic

191 landfill gas mixture and stirred vigorously. The CO_2 sequestration in each samples vial
192 was analyzed by taking gas samples from the head space in different time intervals for a
193 total of 24 hours.

194 • Series 2: These batch tests were conducted to evaluate long-term carbonation potential of
195 each slag type at water holding capacity. For the IHE-9/17 and Riverdale slags, 1 g each
196 of these slag samples were mixed with 20% (w/w) of water and for IHE-3/15 slag, 1 g of
197 slag sample was mixed with 40% (w/w) of water in 125 mL glass vials and purged with
198 synthetic landfill gas mixture. The selected moisture contents corresponded with their
199 water holding capacity. These slag samples were analyzed till they reached their
200 maximum CO_2 sequestration capacity.

201 • Series 3: These batch tests were conducted to evaluate the effect of temperature on CO_2
202 sequestration by the slags. For testing, three 1g sample of BOF slag were mixed with
203 20% (w/w) of water, purged with synthetic landfill gas mixture and were placed in an
204 incubator at controlled constant temperatures of 7 ºC (44.6 ºF), 23 ºC (73.4 ºF) and 54 ºC
205 (129.2 ºF). The temperatures were selected to account for seasonal variations plus the
206 additional heat due to microbial decomposition of landfill waste.

207 All of the batch experiments were performed in triplicate to ensure repeatability. Gas samples
208 from each vial were analyzed by gas chromatography (GC) using an SRI 9300 GC equipped

209 with a thermal conductivity detector (TCD) and CTR-1 column capable of separating CH_4
210 and CO_2.
211
212 *2.4. Column experiments*
213
214 The column experiments were conducted on each BOF slag under humidified, simulated
215 LFG gas mixture conditions. All experiments were performed at room temperature (± 2 ºC) in
216 acrylic glass columns with an inner diameter 2.5 cm and height 30 cm. Each BOF slag sample
217 was mixed with deionized water (to yield moisture content of 10%) and was placed in the
218 column in approximately 5 cm lifts followed by light tamping. The synthetic LFG at a pressure
219 of approximately 40 kPa was passed through a water column to humidify (not measured) the gas
220 before introducing it into the column. Flow meters (Cole-Parmer, Model No. PMRI-010874)
221 were connected at the column inlet and outlet to control the influent gas flow rates (10-12
222 mL/min) and measure the effluent gas flow rate. Gas sampling ports were connected to the inlet
223 and outlet of the columns to allow measurement of the influent and effluent gas concentrations.
224 The experimental set up is shown in **Figure 1**. Gas samples were collected at regular time
225 intervals from inlet and outlet sampling ports and analyzed by SRI 9300 GC. **Table 2** shows the
226 experimental conditions for the column tests.
227

3. Results and discussion

3.1. BOF slag characterization

The physical, geotechnical and chemical properties of the three BOF slags are summarized in **Table 3**. The grain size distribution of the three slags are shown in **Figure 2**, all three slags were dominated by sand-sized particles. The IHE-3/15 slag had the most fines which contributed to an average particle size (0.47 mm) nearly three times smaller than the other slags. The specific gravity of the IHE-3/15 was the lowest which may be attributed to its lower iron content. The water holding capacity (WHC) of the IHE-3/15 slag was twice that of the other slags.

The total elemental content, TCLP and SPLP results for the constituents of concern (COC) metals for all the three BOF slags are presented in **Table 4** and are consistent with the ranges given by Proctor et al. (2000). The TCLP concentrations are below the Resource Conservation and Recovery Act (RCRA) limits demonstrating that the slag is non-hazardous. The major difference between the three slags was the elemental content of aluminum (Al) in the Riverdale slag is about six times more than that of the other slags. Steel slag is a complex mixture and contains many insoluble silicates and other strongly pH buffered minerals.

As such, leaching of the metals is typically low and similar regardless of the total elemental content.

Mineralogically, the slag composition in terms of major oxides and the mineral phases is presented in **Table 5**. IHE-3/15 had lowest Fe content and highest LOI, whereas Riverdale had highest Al content which is consistent with **Table 4**. The major oxides present are consistent with the ranges given by Shi (2004). However, the amount of Al_2O_3 (11.6%) in Riverdale exceeds the range (1-6%) given by Shi (2004). The major mineral phases determined by QXRD were free lime (CaO), portlandite [$Ca(OH)_2$], larnite (Ca_2SiO_4 or C_2S), and calcium ferrite ($Ca_2Fe_2O_5$ or C_2F). The IHE-3/15 slag had the highest amount of free lime and portlandite [CaO + $Ca(OH)_2$] (~12%) nearly double that of IHE-9/17 slag and 3.5 times that of Riverdale slag. The IHE-3/15 slag contained calcite and vaterite (~5.5%) suggesting the sample had undergone certain aging. Studies have shown that CaO and $Ca(OH)_2$ have the highest CO_2 sequestration potential among the various minerals present in the steel slag (Bonenfant et al., 2009; Pan et al., 2012). Calcium silicates hydrates (C-S-H) can also react with CO_2 and form $CaCO_3$ precipitates and a silica gel (Pan et al., 2012). Free lime and portlandite, which are readily water-soluble and strongly buffered, are the first to react and form carbonates followed by other species with lower solubility, like larnite (or C_2S) where Ca is generally bound with silicates (Uibu et al., 2011). The Riverdale slag showed significant amount of calcium aluminate ($Ca_3Al_2O_6$ or C_3A) and tetra-calcium aluminoferrite ($Ca_4Al_2Fe_2O_{10}$ or C_4AF) which renders hydration property to Riverdale slag.

Figure 3 presents the SEM images of the non-carbonated (as-received) and carbonated BOF slags from this study. The as-received BOF slag was observed to have more porous

surfaces and visually discrete as shown in **Figure 3**. The carbonated phase was characterized with the outgrowths in the shape of needles or plates or rods, filling the voids between the particles as shown in **Figure 3** (carbonated). Such outgrowths were identified as carbonates formed during carbonation reactions (Huijgen et al., 2005, Chang et al., 2011).

3.2. Batch experiments: Effect of moisture content on CO_2 sequestration

The results of the first series of batch experiments are presented in **Figures 4**. **Figure 4a** shows CO_2 removal by the three BOF slags at different moisture contents and different points of time until 24 hours. **Figure 4b** shows negligible uptake of CO_2 by all three slags in a dry state (0% moisture) and a significant increase upon addition of the moisture. The optimum moisture content (OMC) for CO_2 sequestration by IHE-3/15 slag was 10% (L/S ratio of 0.1 L/kg) whereas, the OMC for the IHE-9/17 and Riverdale slags was approximately 20% (L/S ratio of 0.2 L/kg). The reason for the lower OMC for the IHE-3/15 slag likely relates to the finer particle size and higher lime/portlandite contents. As shown in **Figure 4b**, the 24-hour CO_2 sequestration capacity of IHE-3/15 slag was the highest (53-68 mg/g) followed by IHE-9/17 (32-45 mg/g) and Riverdale (19-38 mg/g). **Figure 4b** also shows negligible uptake of CO_2 by all three slags in a dry state (0% moisture). **Figures 4c** and **4d** show the amount of CH_4 uptake by each BOF slag; however, it was not very significant (< 6 mg/g).

Figure 4a shows that most of the CO_2 removal occurs in the first 5 hours after which the rate of CO_2 removal was nearly constant in all the moisture content ranges (10% to 20%) across all the three BOF slags tested. This suggests a two-step reaction mechanism for carbonation in BOF slags. The first step likely comprises of the dissolution of free CaO and $Ca(OH)_2$ and reaction with CO_2 as these two minerals are readily soluble and easily carbonated at the natural pH of the BOF slag. The flatter slope of the curves shown in **Figure 4a** (after 5 hours) likely involves other soluble species and potentially slower reaction rate perhaps contributable to the dissolution of C_2S as it is the second most reactive phase after [CaO + $Ca(OH)_2$]. Huijgen et al. (2005) had also reported that Ca silicates have lower carbonation rates than $Ca(OH)_2$ owing to their lower solubility rates. At all the moisture content ranges studied, the IHE-3/15 BOF slag showed the highest CO_2 sequestration capacity which was consistent with the highest [CaO + $Ca(OH)_2$] content.

The results of second series of batch experiments performed at the WHC of each slag [IHE-3/15 (40%), IHE-9/17 (20%), Riverdale (20%)] in an effort to simulate the impact of high rainfall infiltration are shown in **Figure 5**. These results show that the CO_2 removal by the three BOF slags continues to occur over 50 to 66 days. The maximum CO_2 removal capacities were reasonably estimated when the removal curve reached an asymptote. The respective maximum CO_2 removal capacities of IHE-3/15, IHE-9/17 and Riverdale slags were 105 mg/g, 80 mg/g and

305 67 mg/g, respectively. The corresponding reaction times were 1600 hours for IHE-3/15 and 1200
306 hours for IHE-9/17 and Riverdale.

307 Assuming all the CaO and $Ca(OH)_2$ present (as determined by QXRD, see Table 5)
308 would react with CO_2, the theoretical CO_2 removal capacity of the IHE-3/15, IHE-9/17 and
309 Riverdale BOF slags based on stoichiometric considerations would correspond to 72, 32 and 21
310 mg/g, respectively. The maximum amount of CO_2 removed in first 5 hours (**Figure 4a**)
311 corresponds to 54, 34 and 25 mg/g for IHE-3/15, IHE 9/17 and Riverdale slag, respectively,
312 which is consistent with the theoretical CO_2 removal capacity based on [CaO + $Ca(OH)_2$] content
313 of each slag. Hence, it can be hypothesized that CaO and $Ca(OH)_2$ were responsible for initial or
314 primary carbonation reaction.

315 Furthermore, in IHE-9/17 and Riverdale slags, carbonation continued beyond the
316 carbonation capacity of the [CaO + $Ca(OH)_2$] present in the respective slags. This is indicative of
317 the participation of other Ca containing minerals in the carbonation reaction. Huijgen et al.
318 (2005), Bonenfant et al. (2008), Uibu et al. (2011) and Su et al. (2016) have reported, based on
319 the XRD and TGA analysis on the carbonated and non-carbonated slag samples, that after CaO
320 and $Ca(OH)_2$, larnite (C_2S) is the most reactive mineral phase for carbonation. Hence, the
321 carbonation of other Ca containing minerals mainly C_2S or those which dissolve at higher pH
322 can be assumed as the secondary carbonation reaction. The total theoretical CO_2 sequestration
323 potential of IHE-3/15, IHE-9/17 and Riverdale slag based on the amount of [CaO + $Ca(OH)_2$ +

C_2S] corresponds to 126, 93 and 101 mg/g, respectively. The 24 hour CO_2 sequestration by IHE-9/17 and Riverdale slags is consistent with the theoretical capacity of [$CaO + Ca(OH)_2 + C_2S$] which confirms that C_2S or other Ca containing mineral phases were participating in the carbonation reaction.

The CO_2 removed in long-term batch experiments was higher than that of 24-hour batch experiments exhibiting the effect of reaction time on carbonation of the minerals. The minerals which are not readily carbonated or have slower reaction kinetics like C_2S may participate in carbonation with an increase in reaction time. Similarly, the long-term batch experiments also showed higher CO_2 sequestration than the theoretical capacity of [$CaO+ Ca(OH)_2$] which further confirms the participation of C_2S or other Ca containing minerals, including Ca bearing solids comprising the amorphous content (40-50 wt%).

On the other hand, the long term batch experiments results showed that the measured capacity of each respective slag was exhausted before its theoretical CO_2 sequestration capacity [$Ca(OH)_2 + CaO + C_2S$]. The limiting factors could be related to grain size effects, availability of moisture, and development of Ca-depleted silicate rims around the slag particles which limit further leaching of Ca from the inner core of slags (Huijgen et al., 2005, 2006).

Very low CH_4 uptake was observed in all three BOF slags during long-term batch experiments, and the CH_4 uptake was similar (~10 mg/g) indicating a weak dependence on grain size, moisture and mineralogy, despite the elevated alumina content of the Riverdale slag.

343

344 *3.3.Batch experiments: Effect of temperature on CO_2 sequestration*

345

346 Landfill covers are subjected to wide variations of temperature due to the seasonal
347 variations and heat generation from different phases of decomposition of MSW and other
348 inorganic exothermic chemical reactions within the landfill. Landfill temperatures as high as 60-
349 80 ºC has been reported in literature (Hanson et al., 2009; Jafari et al., 2014). The effects of
350 variation of temperature on CO_2 sequestration capacity of BOF slags were examined in batch
351 experiments at 7 ºC, 23 ºC and 54 ºC. **Figure 6** shows the CO_2 removal by the three BOF slags
352 as a function of temperature. The 24-hour CO_2 removal for IHE-3/15 was highest at all the
353 temperatures tested and showed a decreasing trend with increase in temperature which is
354 consistent with the study by Quaghebeur et al. (2015) in which an inverse trend with temperature
355 from 20 ºC to 140 ºC for a BOF slag with high [$CaO + Ca(OH)_2$] content was observed. IHE-
356 9/17 slag did not show any specific trend with temperature, while Riverdale slag showed an
357 increasing trend with increase in temperature (**Figure 6**). The effect of temperature on
358 carbonation is a combination of dissolution rate of minerals as well as CO_2. Solubility of CO_2
359 decreases whereas leaching of Ca from calcium bearing minerals increases with temperature
360 (Huijgen et al., 2005). The solubility of hydroxides ($Ca(OH)_2$ and $Mg(OH)_2$) decrease with
361 increase in temperature (Quaghebeur et al., 2015 and Park et al., 2003). The dissolution of

362 $Ca(OH)_2$ and CO_2 are likely to be the rate limiting factors in case of IHE-3/15 slag at elevated
363 temperature. On the other hand, solubility of silicates may be the rate determining factor in case
364 of Riverdale slag as the solubility of silicates increases with temperature (Quaghebeur et al.,
365 2015). From this study it can be said that the type of minerals and their solubility at different
366 temperature play an important role in CO_2 sequestration.
367
368 *3.4. Column experimental results*
369
370 **Figures 7a and 7b** show the CO_2 and CH_4 sequestration potential of the three BOF slags
371 on a pore volume (PV) basis of gas flow. An initial phase of near complete CO_2 (100%) removal
372 can be seen in **Figure 7a** with breakthrough occurring at different times for different BOF slags
373 (80, 30 and 19 PV or 10, 5 and 2 hours for IHE-3/15, IHE-9/17 and Riverdale, respectively).
374 After breakthrough, the CO_2 removal gradually decreased to nearly 0% which is taken to be the
375 ultimate or operational CO_2 removal capacity of each BOF slag under experimental conditions.
376 A similar CO_2 removal pattern was observed in all three BOF slags after breakthrough as shown
377 in **Figure 7a**. The removal efficiency decreases sharply after breakthrough; however, the
378 removal continues at a slower rate for a longer period leading to considerable uptake of CO_2. The
379 exhaustion or termination time was different for different BOF slags (1,033, 430 and 333 hours
380 for IHE-3/15, IHE-9/17 and Riverdale, respectively). Similarly, termination PVs of inflow gas

were 8,400, 3,600 and 3,200 for IHE-3/15, IHE-9/17 and Riverdale, respectively. IHE-3/15 slag had highest CO_2 removal rates and removal capacity.

Figures 8a and 8b show the cumulative CO_2 and CH_4 sequestered in short and long term, during column experiments with each BOF slag. **Figure 8a** shows the cumulative removal of CO_2 by the three BOF slags in the initial phase of the column experiment when a slope change occurs signifying the change in removal rate. At breakthrough, the amount of CO_2 sequestered was 28, 7 and 4 mg/g for IHE-3/15, IHE-9/17 and Riverdale slag, respectively. The gradual decline in slope after breakthrough can be attributed to the deposition of the carbonate compounds on the slag surface preventing contact of Ca and CO_2. However, with prolonged reaction time, the CO_2 removal progresses at a slower rate which shows that the deposition of carbonate compounds or calcite influences the reaction rate but does not limit the CO_2 sequestration potential of the slag.

IHE-3/15 slag distinctly showed higher CO_2 sequestration than IHE-9/17 and Riverdale slag in column experiments. This suggests that the [CaO, $Ca(OH)_2$ and C_2S] content, particle size, and porosity are the governing factors for CO_2 sequestration. In contrast to IHE-3/15 and IHE-9/17 slags, Riverdale slag showed the presence of significant amount of C_3A and C_4AF whose hydration will compete for available moisture and potentially impact carbonation reactions.

399 **Figure 7b** shows percent removal of CH_4. The BOF slags showed some removal of CH_4
400 in the beginning which was followed by sudden decrease in the removal gradually leading to
401 nearly 0% removal. From **Figures 8a** and **8b**, it can be seen that the CH_4 uptake is relatively low
402 in comparison to CO_2 in all three BOF slags. **Figure 8a** shows initial higher rate of CH_4 removal
403 followed by a nearly constant phase and this pattern is similar in all the three BOF slags. The
404 reason for this behavior could be the adsorption of CH_4 on the surface of the slag particles due to
405 the presence of high alumina content, which is reported to have the potential to adsorb CH_4 (Li et
406 al., 1994a, b). However, Riverdale slag that has the highest alumina content showed the lowest
407 CH_4 removal which suggests that alumina content of the slag may not be contributing
408 significantly towards CH_4 adsorption. Perhaps the slag particle size may have a considerable
409 impact on adsorption of CH_4 since the IHE-3/15 slag showed relatively higher CH_4 removal in
410 comparison to other two slags. Hence, this behavior requires a further detailed investigation for
411 the fundamental reason behind the CH_4 removal in the BOF slags tested.
412 Comparing the CO_2 sequestered until breakthrough with the theoretical capacity of [CaO
413 + $Ca(OH)_2$] in each slag, the carbonate conversion will correspond to 39%, 22% and 19% in
414 IHE-3/15, IHE-9/17 and Riverdale slags, respectively. Considering all the [CaO + $Ca(OH)_2$]
415 would react in the beginning, the breakthrough PV would be 167, 101 and 78 for IHE-3/15, IHE-
416 9/17 and Riverdale slags, respectively. However, the breakthrough occurred at lesser PV than the
417 theoretical PV which suggests that not all the free CaO and $Ca(OH)_2$ were available for

418 carbonation. The steep slope in **Figure 8a** until breakthrough suggests rapid reaction kinetics
419 likely due to the readily available [CaO + $Ca(OH)_2$]. Besides that, the change in slope after
420 breakthrough shows a two-step reaction mechanism: initial rapid reaction followed by slower
421 reaction kinetics. The maximum CO_2 sequestration capacity of IHE-3/15, IHE-9/17 and
422 Riverdale slags as quantified from the column experiments are 325, 85 and 56 mg/g, respectively
423 which correspond to 100%, 91% and 55% conversion of [CaO + $Ca(OH)_2$ + C_2S] present in each
424 BOF slag assuming all of it would react with CO_2. A maximum carbonate conversion of 93.5 %
425 has been reported by Chang et al. (2012) in a high-gravity rotating packed bed at a reaction time
426 of 30 min, rotating speed of 750 rpm and temperature of 65 °C. Similarly, the degree of
427 carbonation achieved in the past studies is shown in Table 1. Studies have reported higher degree
428 of carbonation under high temperature and pressure and for smaller particle size fraction of the
429 slag. In our study, higher degrees of carbonation were achieved under ambient conditions which
430 could be attributed to the prolonged exposure of the slags with the humid LFG mixture.
431 It is noteworthy that despite having similar total [CaO + $Ca(OH)_2$ + C_2S] content and
432 particle size as the IHE-9/17 slag, the Riverdale slag showed lower CO_2 sequestration potential.
433 The reason for this could be the presence of relatively lower [CaO and $Ca(OH)_2$] and higher C_2S
434 content in Riverdale slag than IHE-9/17 slag as Ca silicates have lower carbonation rate than
435 $Ca(OH)_2$ (Huijgen et al., 2005). Other limiting factors for carbonation could be the degree of
436 compaction or in-place density (which leads to different porosities) of the slag in the column that

437 can affect the slag surface available for carbonation. High porosity means more slag surface
438 exposed to inflowing CO_2 gas. The porosity of the Riverdale slag (0.44) was 1.2 times less than
439 that of IHE-9/17 slags. The ultimate CO_2 sequestration of IHE-9/17 slag as measured from the
440 column experiment was 1.5 times that of the Riverdale slag which follows similar relation as
441 obtained in terms of porosity of the slags. It suggests that there could be an influence of porosity
442 on the CO_2 uptake by each BOF slag.
443
444 **4. Conclusions**
445
446 This study evaluated the CO_2 sequestration potential of different BOF slags, from
447 different steel production plants and different production batches, subjected to simulated landfill
448 gas conditions. The CO_2 sequestration of three BOF slags was assessed under varying moisture
449 conditions and temperatures. The characterization of the BOF slags showed that, despite having
450 similar production process, the slags could differ in their physical and chemical properties. The
451 batch experimental results showed that the effect of mineralogy and particle sizes of slags on
452 CO_2 sequestration are more pronounced than that of moisture content and temperature. CaO,
453 $Ca(OH)_2$ and C_2S were found to be the primary minerals responsible for CO_2 sequestration in the
454 slag with [CaO + $Ca(OH)_2$] being the first one to react during carbonation. A two-step reaction

455 mechanism was observed during carbonation with an initial rapid reaction phase followed by a
456 relatively slower reaction rate.

457 In the column experiments, CO_2 sequestration capacity was found to be a function of
458 various parameters like mineralogy, particle size, moisture, and porosity. IHE-3/15 slag, which
459 had highest finer fractions (9.5%), smaller average particle size (0.47mm), highest porosity
460 (57%) and highest [$CaO + Ca(OH)_2$] content (11.5%) among the three BOF slags, showed the
461 highest CO_2 sequestration. Initial phase of complete removal of CO_2 until breakthrough followed
462 by gradual reduction in the rate of CO_2 removal was observed and this behavior was attributed to
463 the carbonation of readily available [$CaO + Ca(OH)_2$] in the beginning followed by other
464 minerals with lower carbonation rates like C_2S. The possibility of participation of the amorphous
465 phase present in the BOF slag in carbonation reaction was also highlighted.

466 Overall, it can be concluded that the BOF slag has significant CO_2 sequestration potential
467 under synthetic landfill gas condition; however, the CO_2 sequestration capacity may vary with
468 the type of BOF slags and other physical parameters. Hence, it is utmost important to understand
469 the characteristics of the BOF slags before implementing them in landfill covers in large scale.

470

471 **Acknowledgements**

472

473 This project is funded by the U.S. National Science Foundation (grant CMMI #
474 1724773), which is gratefully acknowledged. Phoenix Services, LLC, is acknowledged for being
475 an industrial partner on this project and providing slag samples for the experiments.
476

477 **References**

478

479 Baciocchi, R., Costa, G., Polettini, A., and Pomi, R., 2009. Influence of particle size on the
480 carbonation of stainless steel slag for CO_2 storage. Energy Procedia, 1(1), 4859-4866.

481 Bonenfant, D., Kharoune, L., Sauve, S., Hausler, R., Niquette, P., Mimeault, M., and Kharoune,
482 M., 2008. CO_2 sequestration potential of steel slags at ambient pressure and
483 temperature. Ind. Eng. Chem. Res., 47(20), 7610-7616.

484 Belhadj, E., Diliberto, C., and Lecomte, A., 2014. Properties of hydraulic paste of basic oxygen
485 furnace slag. Cem. Concr. Compos., 45, 15-21.

486 Chang, E. E., Chen, C. H., Chen, Y. H., Pan, S. Y., and Chiang, P. C., 2011. Performance
487 evaluation for carbonation of steel-making slags in a slurry reactor. J. Hazard.
488 Mater., 186(1), 558-564.

489 Chang, E. E., Pan, S. Y., Chen, Y. H., Tan, C. S., and Chiang, P. C. 2012. Accelerated
490 carbonation of steelmaking slags in a high-gravity rotating packed bed. J. Hazard. Mater.,
491 227, 97-106.

492 Georgaki, I., Soupios, P., Sakkas, N., Ververidis, F., Trantas, E., Vallianatos, F., and Manios, T.,
493 2008. Evaluating the use of electrical resistivity imaging technique for improving CH_4
494 and CO_2 emission rate estimations in landfills. Sci. Total Environ., 389(2-3), 522-531.

Goldsmith Jr, C. D., Chanton, J., Abichou, T., Swan, N., Green, R., and Hater, G., 2012. Methane emissions from 20 landfills across the United States using vertical radial plume mapping. J. Air Waste Manage. Assoc., 62(2), 183-197.

Hanson, J. L., Yeşiller, N., and Oettle, N. K., 2009. Spatial and temporal temperature distributions in municipal solid waste landfills. J. Environ. Eng., 136(8), 804-814.

Hegde, U., Chang, T. C., and Yang, S. S., 2003. Methane and carbon dioxide emissions from Shan-Chu-Ku landfill site in northern Taiwan. Chemosphere, 52(8), 1275-1285.

Huijgen, W. J., Witkamp, G. J., and Comans, R. N., 2005. Mineral CO_2 sequestration by steel slag carbonation. Environ. Sci. Technol., 39(24), 9676-9682.

Huijgen, W. J., Witkamp, G. J., and Comans, R. N., 2006. Mechanisms of aqueous wollastonite carbonation as a possible CO_2 sequestration process. Chem. Eng. Sci., 61(13), 4242-4251.

Isenburg, J., and Moore, M., 1992. Generalized acid neutralization capacity test. In Stabilization and Solidification of Hazardous, Radioactive, and Mixed Wastes: 2nd Volume. ASTM International.

Jafari, N. H., Stark, T. D., and Rowe, R. K., 2014. Service life of HDPE geomembranes subjected to elevated temperatures. J. Hazard. Toxic Radioact. Waste, 18(1), 16-26.

Ko, M. S., Chen, Y. L., and Jiang, J. H., 2015. Accelerated carbonation of basic oxygen furnace slag and the effects on its mechanical properties. Constr. Build. Mater., 98, 286-293.

Kolani, B., Buffo-Lacarrière, L., Sellier, A., Escadeillas, G., Boutillon, L., and Linger, L., 2012. Hydration of slag-blended cements. Cem. Concr. Compos., 34(9), 1009-1018.

516 Kunzler, C., Alves, N., Pereira, E., Nienczewski, J., Ligabue, R., Einloft, S., and Dullius, J.,
517 2011. CO_2 storage with indirect carbonation using industrial waste. Energy Procedia, 4,
518 1010-1017.

519 Lekakh, S. N., Rawlins, C. H., Robertson, D. G. C., Richards, V. L., and Peaslee, K. D., 2008.
520 Kinetics of aqueous leaching and carbonization of steelmaking slag. Metall. Mater.
521 Trans. B, 39(1), 125-134.

522 Li, C., Yan, W., and Xin, Q., 1994a. Interaction of methane with surface of alumina studied by
523 FT-IR spectroscopy. Catal. Lett., 24(3-4), 249-256.
524 Li, C., Li, G., and Xin, Q., 1994b. FT-IR spectroscopic studies of methane adsorption on
525 magnesium oxide. J. Phys. Chem., 98(7), 1933-1938.

526 Mahoutian, M., Shao, Y., Mucci, A., and Fournier, B., 2015. Carbonation and hydration behavior
527 of EAF and BOF steel slag binders. Mater. Struct., 48(9), 3075-3085.

528 Pan, S. Y., Chang, E. E., and Chiang, P. C., 2012. CO_2 capture by accelerated carbonation of
529 alkaline wastes: a review on its principles and applications. Aerosol Air Qual.
530 Res., 12(5), 770-791.

531 Pan, S. Y., Adhikari, R., Chen, Y. H., Li, P., and Chiang, P. C., 2016. Integrated and innovative
532 steel slag utilization for iron reclamation, green material production and CO_2 fixation via
533 accelerated carbonation. J. Clean. Prod., 137, 617-631.

534 Proctor, D. M., Fehling, K. A., Shay, E. C., Wittenborn, J. L., Green, J. J., Avent, C., and Zak,
535 M. A., 2000. Physical and chemical characteristics of blast furnace, basic oxygen furnace,
536 and electric arc furnace steel industry slags. Environ. Sci. Technol., 34(8), 1576-1582.

537 Quaghebeur, M., Nielsen, P., Horckmans, L., and Van Mechelen, D., 2015. Accelerated
538 carbonation of steel slag compacts: Development of high-strength construction
539 Materials. Frontiers in Energy Research, 3, 52.

540 Reddy, K. R., Gopakumar, A., and Chetri, K. J., 2018a. Critical review of applications of iron
541 and steel slags for carbon sequestration and environmental remediation. Rev. Environ.
542 Sci. Bio. (accepted)

543 Reddy, K. R., Gopakumar, A., Rai, K. R., Kumar, G., Chetri, K. J. and Grubb. D., 2018b. Effect
544 of basic oxygen furnace slag particle size on sequestration of carbon dioxide from landfill
545 gas. Waste Manag. Res. (accepted)

546 Sarfo, P., Das, A., Wyss, G., and Young, C. 2017. Recovery of metal values from copper slag
547 and reuse of residual secondary slag. Waste Manage., 70, 272-281.

548 Shi, C., (2004). Steel slag—its production, processing, characteristics, and cementitious
549 properties. J. Mater. Civ. Eng., 16(3), 230-236.

550 Su, T. H., Yang, H. J., Shau, Y. H., Takazawa, E., and Lee, Y. C., 2016. CO_2 sequestration
551 utilizing basic-oxygen furnace slag: Controlling factors, reaction mechanisms and V–Cr
552 concerns. J. Environ. Sci., 41, 99-111.

553 USEPA, 2018. Municipal solid waste landfills., United States Environmental Protection Agency.
554 Available at <https://www.epa.gov/landfills/municipal-solid-wastelandfills#publications>
555 (accessed on August 5, 2018)

556 USEPA., 2014. Municipal Solid Waste Landfills: Economic Impact Analysis for the Proposed
557 New Subpart to the New Source Performance Standards. U.S. Environmental Protection

Agency Office of Air and Radiation Office of Air Quality Planning and Standards Research Triangle Park, NC 27711

Uibu, M., Kuusik, R., Andreas, L., and Kirsimäe, K., 2011. The CO_2-binding by Ca-Mg-silicates in direct aqueous carbonation of oil shale ash and steel slag. Energy Procedia, 4, 925-932.

van Zomeren, A., Van der Laan, S. R., Kobesen, H. B., Huijgen, W. J., and Comans, R. N., 2011. Changes in mineralogical and leaching properties of converter steel slag resulting from accelerated carbonation at low CO_2 pressure. Waste Manage., 31(11), 2236-2244.

Wang, Z., Huang, G., An, C., Chen, L., and Liu, J. 2016. Removal of copper, zinc and cadmium ions through adsorption on water-quenched blast furnace slag. Desalin. Water Treat., 57(47), 22493-22506.

Table 1: Studies on carbonation of steel slags

Steel slag	Experimental conditions	Objective	Carbonate conversion (based on total Ca content)	Reference
LD	Experimental set up: 450 mL autoclave reactor Particle size: < 38 µm – < 2 mm L/S ratio : 2 to 20 L/kg Stirring rate : 100-2000 rpm CO_2 pressure: 1-30 bar Temperature: 25-225 °C Duration: 2-30 min	Mineral CO_2 sequestration by steel slag	74 %	Huijgen et al. (2005)
BOF	Experimental set up: Glass column (5 cm inner diameter, 20 cm height) Particle size: 2– 3.3 mm L/S ratio : 0.01 to 0.1 L/kg for unsaturated and 0.4 to 2 L/kg for saturated condition Gas: 20% CO_2, 80% Ar CO_2 pressure: 0.2 bar Temperature: 5-90 °C Duration: 8 to 200 hour	Investigate the potential of accelerated carbonation of steel slag, at relatively low CO_2 pressure, to improve pH and leaching properties, mainly of vanadium	48%	van Zomeren et al. (2011)
BOF	Experimental set up: Rotating packed bed Particle size: < 0.088 mm L/S ratio : 20 L/kg Stirring rate : 500-1250 rpm Gas: 99% CO_2 CO_2 pressure: 1 bar Temperature: 25-65 °C Duration: 30 min	To study the accelerated carbonation of steelmaking slags in a high-gravity rotating packed bed	93.5%	Chang et al. (2012)
BOF	Experimental set up: Batch reactor Particle size: < 1 mm and (1-6 mm) L/S ratio : 0, 0.05, 0.2, 0.3, 0.4 and 0.5 L/kg Gas: 50% CO_2, 50% CH_4	To use industrial by-product as a sorbent to remove CO_2 and H_2S from biogas	18%	Sarperi et al. (2014)

	Stirring rate: 300 rpm Temperature: 20 °C Duration: 24 hour			
BOF	Experimental set up: Rotatory kiln made of stainless steel Particle size: <3.5mm, 3.5-7mm, 7-15mm,15-25mm Relative humidity: 0-80% CO_2 content: 0-40% Temperature: 25-250 °C Duration: 24 hour	Accelerated carbonation of BOF slag and the effect of carbonation on its mechanical properties	12%	Ko et al. (2015)
EAF , BOF and EAF mixed	Experimental set up: Pressure chamber Specimen: rectangular slag panels Gas: 99.5% CO_2 Temperature: Room temperature Pressure: 0.15 MPa Duration: 2 and 24 hour	Examination of carbonation and hydraulic behavior of EAF and BOF slag	-	Mahoutian et al. (2015)
BOF	Experimental set up: 20 mL capped stainless steel cell contained in a 500 mL stainless steel autoclave Particle size: <0.5mm– 3.5mm L/S ratio : 0, 2, 5 and 10 L/kg CO_2 pressure:0-245 bar Temperature: 25-100 °C Duration: 0 to 96 hour	Optimization of carbonation condition , address carbonation mechanism and evaluate the extents of V and Cr release	71%	Su et al. (2016)
BOF	Experimental set up: glass column 2.5 cm inner diameter, 30 cm height Particle size: as received (mean particle size ranging from 0.47 – 1.5 mm) L/S ratio : 0.1 L/kg Gas: Continuous, humid, 50% CO_2 and 50% CH_4 (v/v) CO_2 pressure: < 0.4 bar Temperature: Room temperature Duration : Until steel slag reaches ~0% CO_2 uptake capacity	To examine the effect of BOF slag types on the CO_2 sequestration potential of slag under landfill condition	~100%	Current study

Table 2: Summary of column experimental conditions

Parameters	**IHE-3/15**	**IHE-9/17**	**Riverdale**
Test conditions			
Inlet gas:			
Carbon dioxide (%)	50	50	50
Methane (%)	50	50	50
Moisture condition	Humid	Humid	Humid
Mode of injection	Continuous	Continuous	Continuous
***Column*:**			
Diameter (cm)	2.5	2.5	2.5
Length (cm)	30	30	30
BOF slag mass (g)	187	254	293.5
Average slag particle size (mm)	0.5	1.5	1.5
Moisture content (%)	10	10	10
Dry density (g/cm^3)	1.3	1.67	1.93
Porosity (v/v)	0.58	0.52	0.44
Pore volume (PV, mL)	83	78	68
Inlet flow rate (mL/min)	9-12	9-12	9-12
Inlet pressure (psi)	<6	<6	<6
Outlet flow rate (mL/min)	2-12	2-12	2-12

Table 3: Physical, geotechnical and chemical properties of the BOF slags

Properties	ASTM Method	IHE-3/15	IHE-9/17	Riverdale
Specific Gravity	D854	3.04	3.46	3.46
Grain Size Distribution:	D422			
Gravel (%)		0	20.8	15.7
Sand (%)		90.5	74.2	80.9
Fines (%)		9.5	5.0	3.4
D_{50} (mm)		0.47	1.5	1.5
C_c		0.55	0.7	1.1
C_u		11.92	18	11.6
Atterberg Limits:	D4318			
Liquid Limit (%)		Non-Plastic	Non-Plastic	Non-Plastic
Plastic Limit (%)				
Plasticity Index (%)				
USCS Classification	D2487	SP-SM	SP-SM	SW
Water Holding Capacity (w/w)	D2980	40.5	20	20
Dry Density (g/cm^3)		1.62	1.72	1.90
Hydraulic Conductivity (cm/s)	D2434	4.2×10^{-4}	1.1×10^{-3}	4.1×10^{-4}
Loss on Ignition (%)	D2974	2.5	1.6	0.8
pH (L/S = 1:1)	D4972	12.4	12.1	12.1
Electrical Conductivity (mS/cm)	D4972	6.68	13.3	14.2
Redox Potential (mV)	D4972	-317.9	-313.3	-314.1
ANC (Equivalents of acid/Kg)	STP-1123	6-7	6-7	5-6
Carbonate content (%)	D4373	17	10	8
Elemental Analysis	XRF			
Ca (%)		48.85	40.35	40.85
Fe (%)		21.8	30.25	28.15
Si (%)		12.65	9.55	7.3
Mg (%)		5.6	10.9	9.25
Mn (%)		2.4	2.2	3.25
Al (%)		3.8	3.95	8.35

Table 4: Characteristic leaching properties of the BOF slags

Metals	RCRA limit (mg/L)	Total (mg/kg)			TCLP (mg/L)			SPLP (mg/L)		
		IHE-3/15	IHE-9/17	Riverdale	IHE-3/15	IHE-9/17	Riverdale	IHE-3/15	IHE-9/17	Riverdale
Aluminum		11,000	15,000-19,000	64,000-69,000	0.62	<1.0	70-86	0.16	0.19	0.49-0.76
Antimony		<0.76	<1.7	<1.7	<0.00031	< 0.015	< 0.015	< 0.00016	< 0.0060	< 0.0060
Arsenic	5	1.3	1.7-1.8	5.3-7.6	0.00087	< 0.010	< 0.010	0.00029	< 0.0040	< 0.0040
Barium	100	36	66-72	120-130	0.14	0.13-0.15	0.21-0.25	0.12	0.078-0.083	0.19-0.20
Beryllium		<0.76	0.51-0.55	0.45-0.46	<0.00025	< 0.0050	< 0.0050	<0.00013	<0.002	< 0.0020
Boron		330	32-38	55-64	0.12	< 0.23	<0.2 4	0.027	0.08-0.084	< 0.20
Cadmium	1	2.5	<0.42	0.49-0.51	0.00028	< 0.0050	< 0.0050	0.00015	<0.002	< 0.0020
Calcium		290,000	220,000-260,000	280,000-310,000	2,300	2,200-2,600	1,500-1,600	800	880-1,000	590-900
Chromium	5	1,100	1,300-1,400	1,600	0.011	0.029-0.045	<0.01-0.016	0.002	0.010-0.011	0.0012-0.0073
Cobalt		1.2	1.4-1.6	1.7-2.4	0.0034	<0.010	< 0.010	0.0013	< 0.0040	< 0.0040
Copper		7.4	9.6-11	21-31	0.005	<0.1	< 0.10	0.0025	< 0.020	< 0.020
Iron		210,000	150,000-180,000	150,000-180,000	0.031	7.8-9.4	<0.25	0.011	3.6-3.8	1.2-1.5
Lead	5	<0.76	2.5-2.7	4.9	0.00041	<0.005	<0.005	0.0002	< 0.0020	< 0.0020
Magnesium		54,000	72,000-79,000	73,000-75,000	0.077	0.29-0.35	<0.25	0.05	< 0.40	< 0.40
Manganese		20,000	13,000-15,000	19,000-20,000	0.005	<0.01	<0.01	0.00072	< 0.0040	0.0040-0.0049
Mercury	0.2	<0.01	<0.019	<0.017	0.00005	<0.0002	<0.0002	0.00005	< 0.00020	-
Nickel		8.2	5.9-6.2	11-13	0.036	0.025-0.03	<0.02	0.013	0.0094-0.0098	<0.008
Potassium		2,000	150-160	49-53	0.76	0.87-1.0	<0.25	0.66	0.48-0.56	0.22-0.44
Selenium	1	<1.2	<0.85	<0.84	0.0047	<0.01	<0.01	0.0019	< 0.0040	< 0.0040
Silver	5	<0.76	<0.85	<0.84	0.00025	< 0.010	< 0.010	0.00013	< 0.0040	< 0.0040
Thallium		<0.23	<0.85	<0.84	0.00025	< 0.0050	< 0.0050	0.00013	< 0.0020	< 0.0020
Tin		-	<4.2	8.8-12	-	< 0.050	< 0.050	-	< 0.020	< 0.020
Vanadium		700	860-970	830-840	0.0058	0.01-0.015	<0.01	0.00078	< 0.0040	< 0.0040
Zinc		59	35-41	50-54	0.035	<0.05	<0.05	0.024	< 0.020	< 0.020

Table 5: Mineralogy and bulk chemistry (oxide basis) of the BOF slags

Minerals and oxides	Mineral formula	BOF Slag		
		IHE-3/15 (wt %)	IHE-9/17 (wt %)	Riverdale (wt %)
Oxide basis				
CaO		33.7	29	40.3
SiO_2		13.35	10.55	10.9
Al_2O_3		3.6	3.8	11.6
Fe_2O_3		15.4	22.25	28.3
MgO		3.1	9.3	10.8
SO_3		0.3	0.2	0.6
LOI		8.6	3.65	0.55
Minerals				
Lime	CaO	2.0-2.2	2.4	1-1.2
Portlandite	$Ca(OH)_2$	9.4-9.5	0-4.4	2-2.3
Larnite	Ca_2SiO_4	9.5-11.4	11.7-12.6	14.5-16.6
Calcite	$CaCO_3$	2.8-2.9	0.8-1.1	0.9-1.3
Vaterite	$CaCO_3$	1.8-2.7	-	-
Srebrodolskite	$Ca_2Fe_2O_5$	6.6-7.8	14.2-15	-
Brownmillerite	$Ca_4Al_2Fe_2O_{10}$	-	-	9-10.4
Calcium Aluminate (C3A)	$Ca_3Al_2O_6$	-	-	6.2-6.4
Bredigite	$Ca_7Mg(SiO_4)_4$	-	-	2.6-1.9
Magnesioferrite	$MgFe_2O_4$	3.3-3.8	6-6.5	4.6-4.9
Iron Magnesium Oxide	Fe0.76Mg0.24O	1.4-1.7	5.2-5.4	3.5-3.8
Wuestite	FeO	2.5-2.7	3.4-3.5	1.7-2.2
Periclase	MgO	0.4-0.6	0.7-0.8	2.7-2.8
Brucite	$Mg(OH)_2$	0.3-0.6	0.4	-
Mayenite	$Ca_{12}Al_{14}O_{33}$	2.7-2.9	2-2.9	3.1-3.3
Akermanite	$Ca_2MgSi_2O_7$	0.0-6.4	2	-
Merwinite	$Ca_3Mg(SiO4)_2$	0.9	1.8-2.1	-
Katoite	$Ca_3Al_2(OH)_{12}$	3.8-4.3	1.7-1.8	1.3-1.5
Quartz	SiO_2	0.3-0.4	-	-
Amorphous Material		41.7-50.1	43-43.7	40.6-46.1

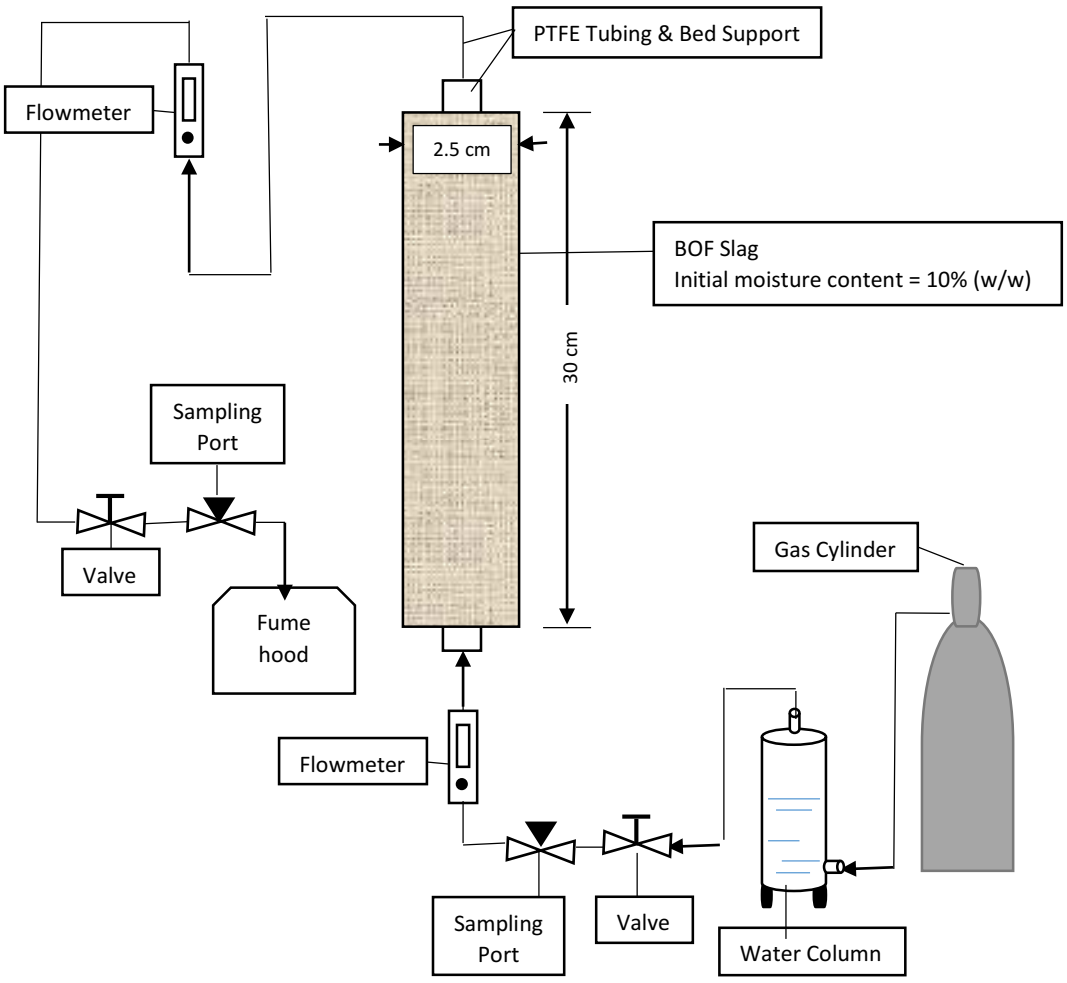

(a)

(b)

Figure 1: Column experimental setup (with humid gas): (a) Schematic; and (b) Photograph.

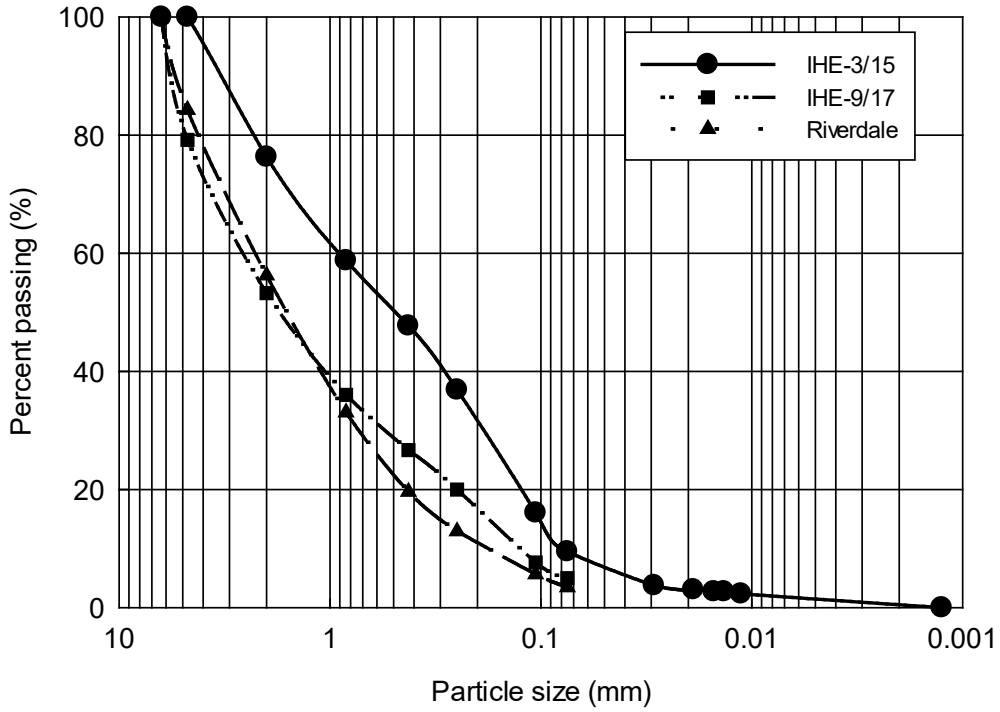

Figure 2: Particle size distribution of the BOF slags (IHE-3/15, IHE-9/17 and Riverdale)

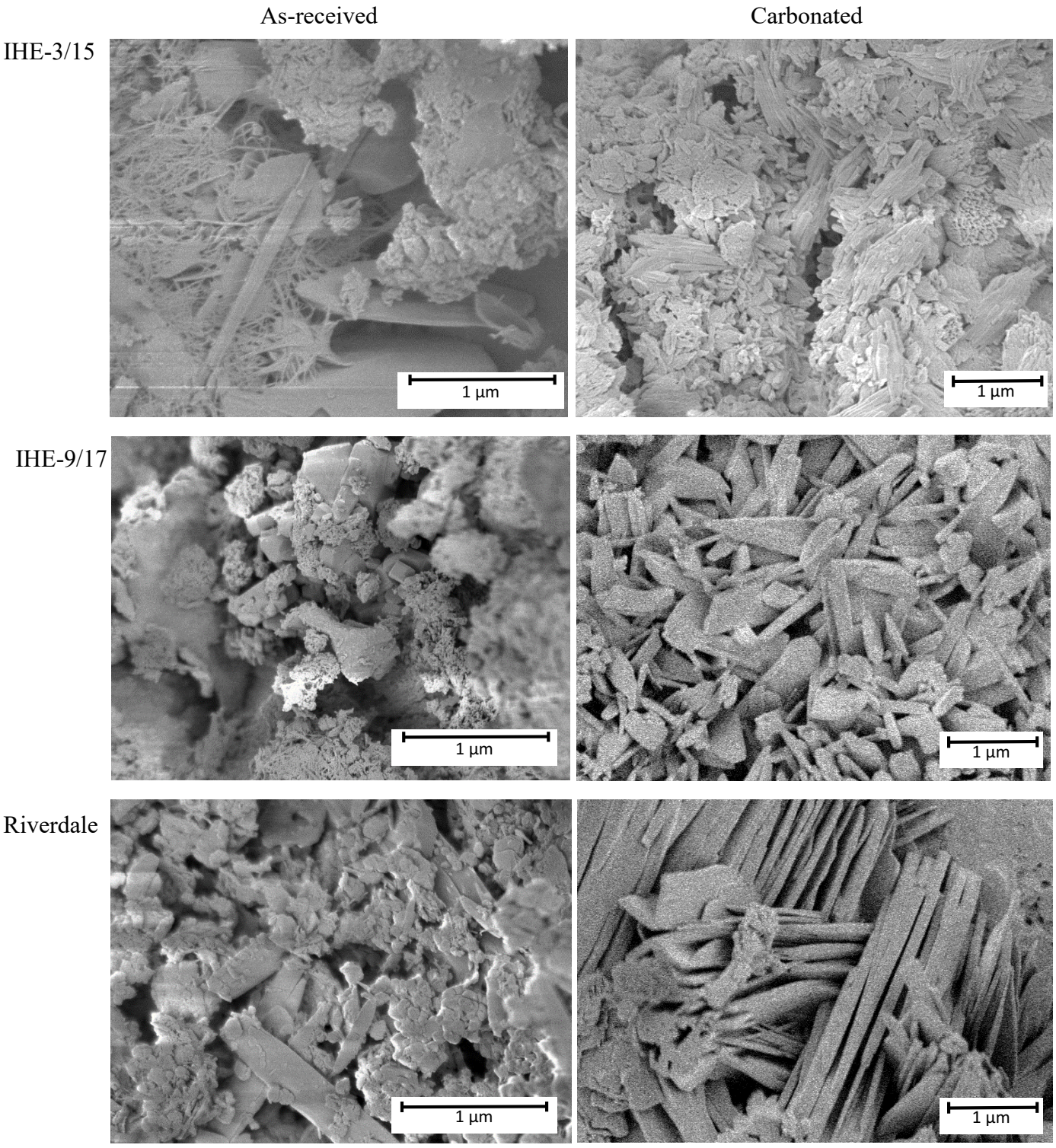

Figure 3: SEM images of as-received and carbonated BOF slags (IHE-3/15, IHE-9/17 and Riverdale)

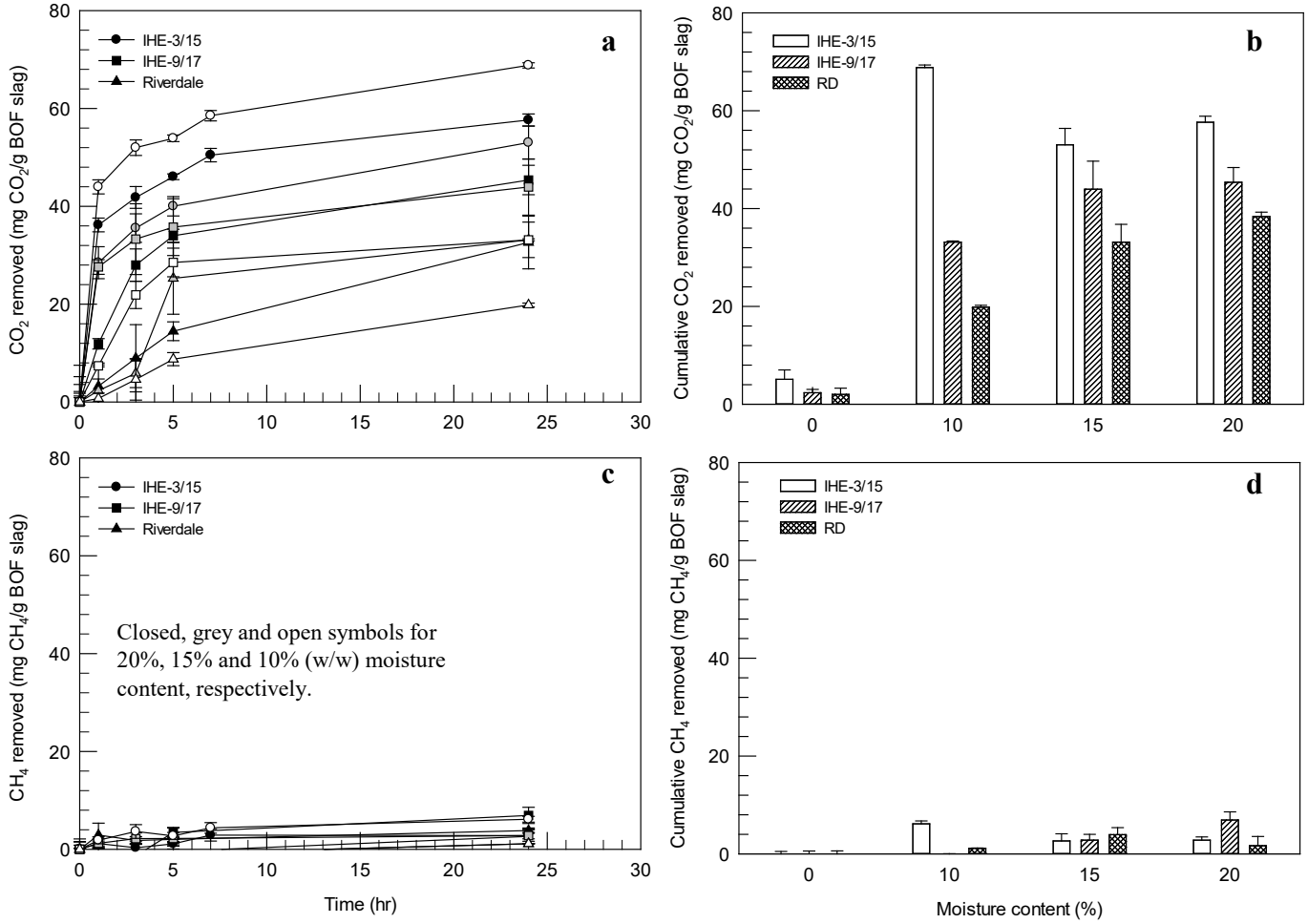

Figure 4: Removal of CO_2 a) hourly and b) cumulative and CH_4 c) hourly and d) cumulative in 24 hours by the BOF slags (IHE-3/15, IHE-9/17 and Riverdale) at different moisture content and exposed to synthetic LFG (50% CO_2:50% CH_4 (v/v)) at room temperature and atmospheric pressure

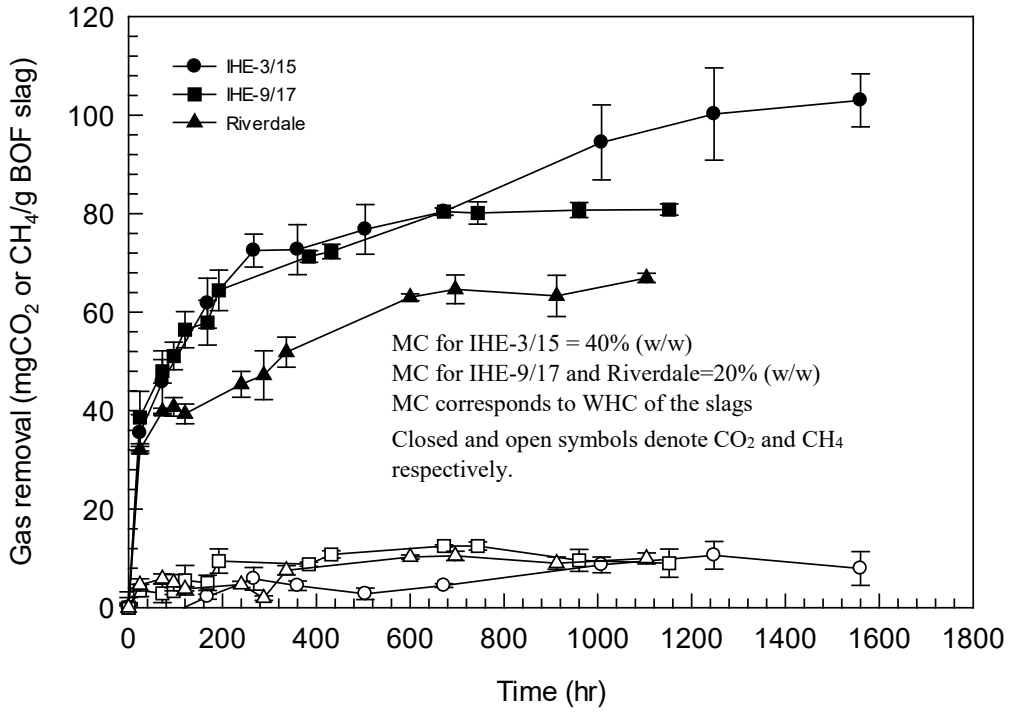

Figure 5: Cumulative removal of CO_2 and CH_4 with time by BOF slags (IHE-3/15, IHE-9/17 and Riverdale) exposed to synthetic LFG (50% CO_2:50% CH_4 (v/v)) at room temperature and atmospheric pressure and moisture content corresponding to the water holding capacity (WHC) of each BOF slag.

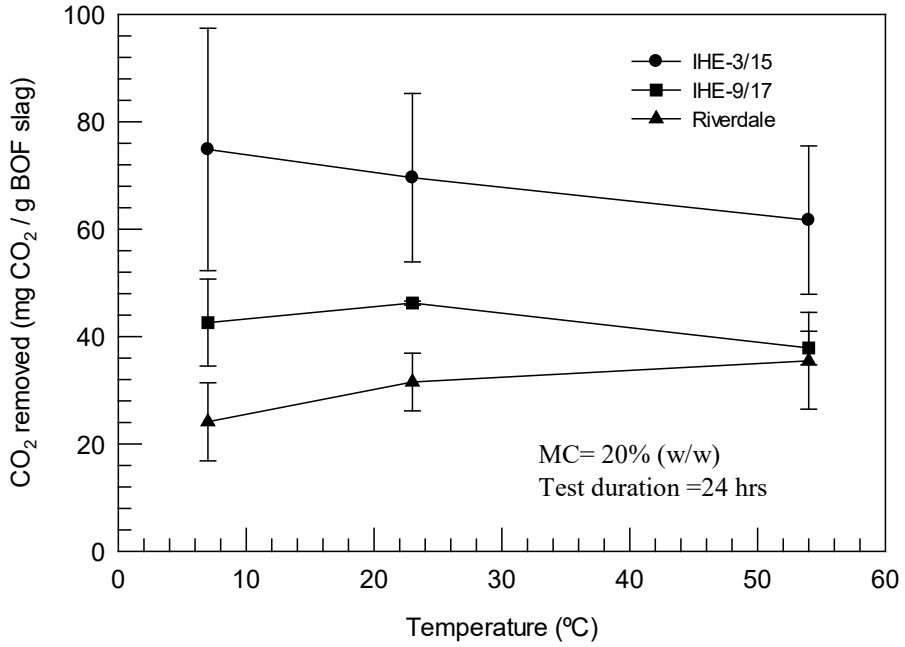

Figure 6: Removal of CO_2 by BOF slags (IHE-3/15, IHE-9/17 and Riverdale) in 24 hours as a function of temperature when exposed to synthetic LFG (50% CO_2:50% CH_4 (v/v)) at an initial moisture content of 20% and atmospheric pressure.

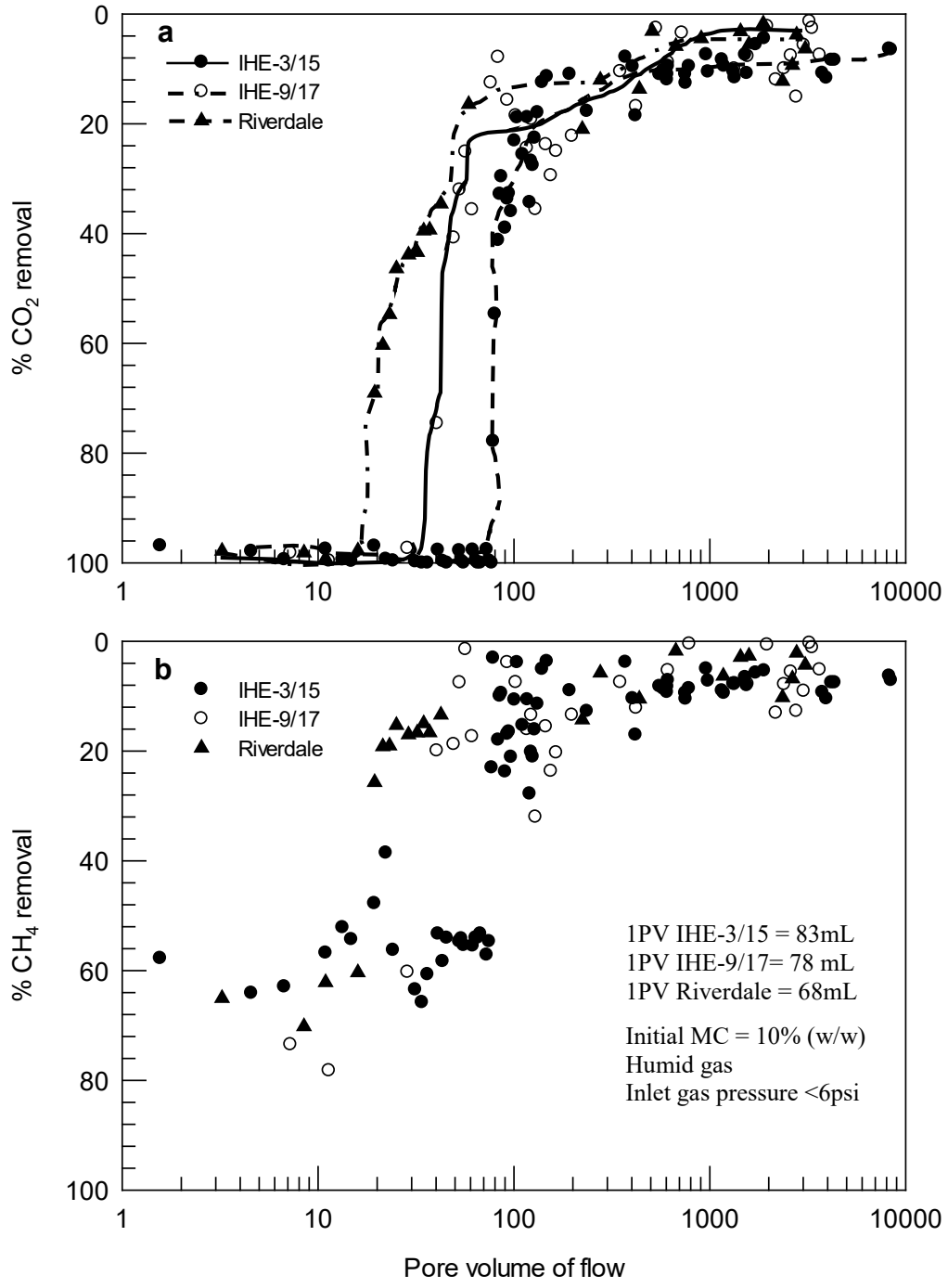

Figure 7: Comparison of percent removal of a) CO_2 and b) CH_4 by BOF slags (IHE-3/15, IHE-9/17 and Riverdale) on a pore volume basis for simulated LFG gas flow (50/50 CH_4/CO_2) at 23 ±2°C.

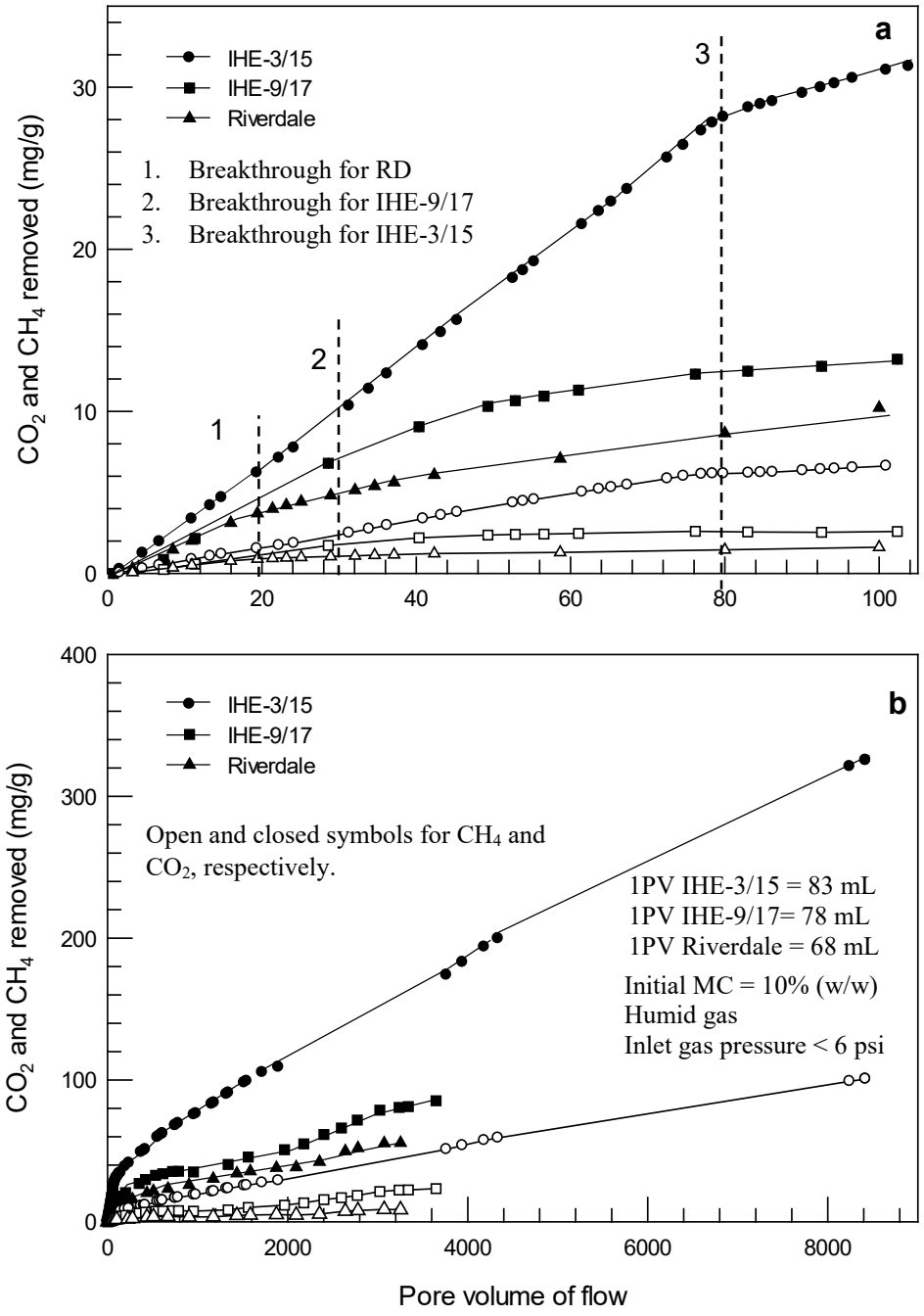

Figure 8: Short (a) and long (b) term CO_2 and CH_4 removal by BOF slags (IHE-3/15, IHE-9/17 and Riverdale) on a pore volume basis for simulated LFG gas flow (50/50 CH_4/CO_2) at 23 ±2°C.